RGS17, an Overexpressed Gene in Human Lung and Prostate Cancer, Induces Tumor Cell Proliferation Through the Cyclic AMP-PKA-CREB Pathway

Michael A. James, Yan Lu, Yan Liu, Haris G. Vikis, and Ming You

Department of Surgery, Washington University School of Medicine, St. Louis, Missouri

Abstract

We have identified RGS17 as a commonly induced gene in lung and prostate tumors. Through microarray and gene expression analysis, we show that expression of RGS17 is up-regulated in 80% of lung tumors, and also up-regulated in prostate tumors. Through knockdown and overexpression of RGS17 in tumor cells, we show that RGS17 confers a proliferative phenotype and is required for the maintenance of the proliferative potential of tumor cells. We show through exon microarray, transcript analysis, and functional assays that RGS17 promotes cyclic AMP (cAMP)-responsive element binding protein (CREB)-responsive gene expression, increases cAMP levels, and enhances forskolin-mediated cAMP production. Furthermore, inhibition of cAMP-dependent kinase prevents tumor cell proliferation, and proliferation is partially rescued by RGS17 overexpression. In the present study, we show a role for RGS17 in the maintenance of tumor cell proliferation through induction of cAMP signaling and CREB phosphorylation. The prevalence of the induction of RGS17 in tumor tissues of various types further implicates its importance in the maintenance of tumor growth. [Cancer Res 2009;69(5):2108–16]

Introduction

Recent evidence has linked regulator of G-protein signaling (RGS) family members to a variety of cancers. RGS1 was shown to be overexpressed in melanoma and its expression found to be significantly associated with decreased relapse-free survival (1). Variants of the RGS domain containing protein PDZ-RhoGEF have been found to modulate the risk of lung cancer in Mexican Americans (2). Another study identified a functional polymorphism in the *RGS6* gene that is associated with bladder cancer risk (3). Recently, we identified *RGS17* as the major candidate for the familial lung cancer susceptibility locus on chromosome 6q23-25.[1] In our analysis of published microarray data comparing normal and tumor tissues, we show that *RGS17* is frequently up-regulated gene in lung and prostate tumors.

RGS17 is a the most recently described member of the RZ subfamily of the RGS family of proteins, and inhibits G-protein–coupled receptor signaling by binding and activating GTPase activity of G(i/o), G(z), and G(q), but not G(s) (4). G(i) and G(s) are named for their inhibitory and stimulatory activity on adenylate cyclase and cyclic-AMP (cAMP) formation. RGS modulation of either G(i)-coupled or G(s)-coupled signaling can therefore enhance or inhibit cAMP formation, respectively (5). Downstream of cAMP, cAMP-dependent protein kinase A (PKA), is activated, which can in turn activate downstream effectors such as cAMP-responsive element binding protein (CREB) and nuclear factor-κB (NFκB). This signaling pathway is best studied for its function in the brain. At least five RGS17 transcripts differing in their noncoding regions and coding for a single detectable protein are expressed in the brain with the highest levels found in the cerebellum (6). Low levels of for RGS17 transcript are detectable in various other peripheral tissues including the lung (6). Although specific functions of RGS17 in the brain are unclear, RGS17 is known to complex with μ-opioid receptors and modulate morphine desensitization through G(z) (7). RGS17 is also known to abrogate μ-opioid–induced cAMP inhibition through an interaction with Protein Kinase C Interacting Protein (8).

In the current study, we find that RGS17 expression is induced in 80% of lung tumors by an average of 8.3-fold in lung cancer of several histologic types, and is also increased in prostate tumors. Knockdown of RGS17 transcript in lung, colon, and prostate tumor cell lines resulted in decreased growth rates in culture and decreased growth of xenografted tumors, whereas overexpression of RGS17 resulted in increased growth rate in lung tumor cells. Microarray gene expression results indicated that RGS17 regulates the expression of central nervous system (CNS) associated genes involved in receptor-mediated signaling and cAMP response. Loss of RGS17 resulted in loss of cAMP and phospho-CREB accumulation as well as loss of forskolin-induced (activator of adenylate cyclase) cAMP formation and forskolin-induced growth stimulation. RGS17 overexpresion partially protected H1299 cells from growth arrest induced by treatment under low serum with H89, a specific inhibitor cAMP-dependent PKA. These novel results implicate RGS17 as a cAMP pathway stimulating inducer of lung tumor growth and implicate RGS17 and the cAMP pathway as therapeutic targets for lung cancer.

Materials and Methods

Quantitative real-time PCR. RNA from paired tumors and normal tissues was obtained from the Tissue Procurement Core at Washington University in St. Louis. cDNA from normal human tissues was obtained from BD Biosciences. Quantitative real-time PCR (qRT-PCR) was conducted using the method as described previously (9). Briefly, 2 μg of total RNA per sample were converted to cDNA using the SuperScript First-Strand Synthesis system for RT-PCR (Invitrogen). Quantitative reverse- trascribed

Note: Supplementary data for this article are available at Cancer Research Online (http://cancerres.aacrjournals.org/).

Requests for reprints: Ming You, Washington University, 660 South Euclid Avenue, 4950 Children's Place, St. Louis, MO 63110. Phone: 314-362-9294; Fax: 314-362-9366; E-mail: youm@wudosis.wustl.edu.

doi:10.1158/0008-5472.CAN-08-3495

[1] M. You et al. Clin Cancer Res. In press 2009.

PCR (RT-PCR) assay was done using the SYBR Green PCR Master Mix (Applied Biosystems). One microliter of cDNA was added to a 25 μL total volume reaction mixture containing water, SYBR Green PCR Master Mix, and primers. Each real-time assay was done in duplicate on a Bio-Rad MyIQ machine. Data were collected and analyzed with Stratagene Mx3000 software. Gene β-actin was used as an internal control to compute the relative expression level (ΔC_T) for each sample. The fold change of gene expression in tumor tissues compared with the paired normal tissues was calculated as 2^d, where $d = \Delta C_{T\ normal} - \Delta C_{T\ tumor}$. One-tailed Student's t test was carried out to assess the overall statistical significance of the difference in gene expression levels between the paired tumor and normal tissues.

Cell culture, overexpression, and RNAi knockdown. HBEC3KT cells were a gift from John Minna (Hamon Center for Therapeutic Oncology Research, University of Texas Southwestern Medical Center, Dallas, TX) and were cultured in Keratinocyte Serum-Free Media (Life Technologies) containing 50 mg/mL bovine pituitary extract (Life Technologies) and 5 ng/mL epidermal growth factor (EGF; Life Technologies). The tumor cell lines H1299 was cultured in RPMI 1640 plus 10% fetal bovine serum (FBS; Life Technologies), and lines DU145 and Hct116 were cultured in DMEM plus 10% FBS (Life Technologies). Cells were transduced with a lentiviral short-hairpin RNA (shRNA) construct based on the pLKo1 vector and designed to specifically target RGS17 transcripts (Open Biosystems). Empty vector control containing an 18 bp stuffer sequence with no knockdown or vector knocking down RGS17 transcript were first packaged in Phoenix cells (Orbigen) and then transduced into target cells with 8 ug/mL Polybrene (Sigma). Medium was replaced 24 h after transduction, and cells were split 1:4 48 h after transduction. At 72 h posttransduction, cells harboring lentiviral constructs were selected with 1 μg/mL puromycin for 2 to 4 d, until mock-infected cells were dead. Surviving cells were pooled and plated at the indicated densities. For overexpression, a NH_2-terminal three hemagglutinin-tagged full-length RGS17 cDNA or the 3HA tag alone was cloned into pCDNA3 for expression of HA-tagged RGS17 protein. Cells at ~60% confluence were transfected with 8 μg of vector with 3HA alone or that expressing 3HA-RGS17 using Geneporter II reagents (Gene Therapy Systems) without serum for 4 h. Serum was added, cells incubated overnight, medium was replaced, and cells were split 1:4 on 2ug/mL puromycin. Cells were selected for 3 d until mock-transfected cells were dead. Cells were pooled and plated at the indicated densities. Cells were treated with 30 μmol/L forskolin (Sigma) or DMSO solvent, and 10 μmol/L IBMX (Sigma) or ethanol solvent. DMSO concentration was <0.2%. H89 stock was dissolved in molecular grade water and added to media at a concentration of 50 μmol/L. Treatment of cells was carried out in medium with the indicated concentration of FBS and drugs, sterile filtered, and applied to cells for the indicated times.

3-(4,5-Dimethylthiazol-2-yl)-2,5-diphenyltetrazolium bromide proliferation assay. Cells were seeded onto 6-well tissue culture dishes at a density of 500 cells per well. Cells were treated with 30 μmol/L forskolin (Sigma) or DMSO solvent, and 10 μmol/L IBMX (Sigma) or ethanol solvent. DMSO concentration was <0.2%. Cells were assayed for viable cell numbers in triplicate using the 3-(4,5-dimethylthiazol-2-yl)-2,5-diphenyltetrazolium bromide (MTT)-based CellTiter 96 Non-Radioactive or AQueous One Solution Cell Proliferation Assay kits (Promega), and A570 or A490, respectively, measured on a plate reader periodically over 6 to 11 d in culture. Medium and drugs were replaced every 3 d. For % viability assays using PKA inhibitor, 5×10^4 cells were seeded into each well of a 12-well tissue culture dish. Starting MTT assay was performed after cell attachment overnight. Cells were treated with 50 μmol/L H89 (Sigma) in medium containing 1% serum and monitored for MTT reduction activity at 1 and 3 d in culture. P values were determined by one-tailed Student's t test.

Colony formation assay. Cells infected with and selected for lentiviral vector control or that expressing shRNA-targeting RGS17 were counted and plated at a density of 100 cells per 100 mmol/L tissue culture dish. After 14 d in culture, medium was removed; cells were stained with crystal violet and photographed.

Nude mouse tumorigenesis assay. Tumor cells stably expressing shRNA vectors as described above were cultured, counted, and resuspended in serum-free medium at a concentration of 1.5×10^7 cells/mL. A volume of 200 μL (3×10^6 cells, respectively) were injected s.c. into the right (vector) or left (shRNA) flank of athymic nude mice at an age of 4 to 6 wk. The health of these mice was monitored thrice weekly and tumor sizes were measured periodically until sacrifice at 2 to 4 wk postinjection depending on the growth rate of the tumors. Tumor volume was determined by the formula ($l \times w \times h$). P values were determined by one-tailed Student's t test.

Microarray. Total RNA was collected by Tri-zol reagent (Invitrogen). RNA was normalized by spectrophotometric reading at 260 nm, aliquoted in triplicate, and submitted to the Vanderbilt Shared Microarray Resource for quality assurance and array analysis of technical triplicates of the biological triplicates H1299 shRGS-1, H1299 shRGS-2, and Hct116 shRGS-2. The 15 input CEL files were analyzed with the Affymetrix HumanExon10ST array to identify genes that were significantly differentially expressed or displayed significant differential alternative splicing between the groups of interest. The input files were normalized with full quantile normalization. Next, the 6553600 probes were manipulated into the analysis values as follows. Probes with GC count <6 and >17 were excluded from the analysis. Nonexpressed probes can cause tests for alternative splicing to find false positives (because they cause "nonparallel" expression patterns across the gene). Hence, a one-sided t test was used to identify probes that are significantly expressed above background probes of similar GC-content (i.e., we reject the null-hypothesis that the probe is not expressed above background if the P value is <0.05). The background probes are defined in the file antigenomic.bgp which is distributed by Affymetrix.[2] Probe scores were then transformed by taking the Natural Logarithm of one plus the probe score. Each probe score was corrected for background by subtracting the median expression score of background probes of similar GC content from the same chip. Probe-sets not significantly expressed above background ($P > 0.05$) are removed from analysis. Probe-set P value is derived via Fisher P value combination. Hence, accept a probe set and reject the hypothesis that it has the same average expression as background if -2 * Sum(Ln(probe DABG P value)) > critical value of χ^2 (level 0.05, d.f. 2* Num_probes_In_Probe-set). Analysis of six published array data sets was performed to identify genes that are coexpressed with RGS17 in lung tumors. We did a general regression test for each individual data set. We also did linear mixed model test for three Affymetrix data sets and three cDNA array data sets separately. To determine expression of RGS17 in tumor tissue compared with normal control tissue, gene expression profiles for RGS17 in five data sets was analyzed as follows: E-MEXP-231 and E-TABM-15[3] and GSE1037, GSE2088, and GSE3325.[4] Relative expression of RGS17 in normal tissues was determined using data from published expression array data set GSE1133.[4]

cAMP assays. cAMP activity was measured in cells pretreated for 20 min with 1 μmol/L IBMX (Sigma) with or without 1 μmol/L apomorphine (Sigma) treatment for 30 min using the Camp-Glo kit (Promega). Levels of cAMP were measured in cells serum starved in 1% FBS containing media for 2 h, pretreated with 1 μmol/L IBMX for 20 min and treatment with 30 μmol/L forskolin (Sigma) or DMSO solvent for 30 min using the Camp-Screen kit (Tropix). DMSO concentration was <0.2%. P values were determined by one-tailed Student's t test.

Western blotting. Cells in each well of 6-well plates were lysed with 250 μL of 1× sample buffer containing cocktailed phosphatase and proteinase inhibitors, sonicated, and then boiled for 10 min. 20 μL was resolved on SDS-PAGE and immunoblotting analyzed with indicated antibodies. Twelve-hour treatment: 80% confluent cells were drug treated with or without 50 μmol/L H-89 on 1% FBS for 12 h, then lysed. Four-day treatment: Cells were treated for 4 d, at which point cells were 50% to 80% confluent and were lysed. Band intensities were measured using Image J software, a public domain application from NIH.

[2] http://www.affymetrix.com
[3] http://www.ebi.ac.uk/arrayexpress
[4] http://www.ncbi.nlm.nih.gov/projects/geo/

Results

Increased expression of RGS17 in tumor tissues. In four published microarray expression data set representing 161 lung tumors and 76 controls, we found RGS17 to be highly expressed in lung tumor tissue (Fig. 1*A*). We also analyzed 1 published data set representing 13 prostate tumors and 6 controls, in which RGS17 also displayed increased expression in tumors compared with normal tissues (Fig. 1*A*). To detect expression of RGS17 in multiple tumor types, RGS17 transcript level in tumor tissues and patient-matched normal tissues was measured by qRT-PCR. In analysis of 61 lung tumors of various pathologies, RGS17 transcript was increased in 80% of lung tumors by an average of 8.3-fold ($P = 1.36 \times 10^{-9}$) over matched normal lung tissue (Fig. 1*B*). RGS17 transcript accumulation was also increased in all of 5 prostate tumors tested by an average of 7.5-fold ($P < 0.02$; Fig. 1*B*). Expression profiles for disease states as suggested by EST counts in published data from National Center for Biotechnology Information's UniGene database[5] show increased expression in lung, breast, and soft tissue tumors (19, 31, and 39 transcripts per million, respectively, compared with 5 transcripts per million in normal tissue). By analysis of a published array data set, we found RGS17 to be expressed predominantly in brain tissues and at relatively low levels in the normal prostate, lung, and bronchial epithelium (Supplementary Fig. S1*A*). Lung tumor cells in culture express higher levels of RGS17 than nontumorigenic immortalized bronchial epithelium (Supplementary Fig. S1*B*). These observations led us to investigate potential oncogenic properties of RGS17 on lung tumor and other tumor cell lines in cell culture and tumorigenesis studies.

RGS17 is required for maintenance of proliferation and tumorigenesis of tumor cell lines. RGS17 transcripts were targeted for knockdown in tumor cell lines from multiple tissue types, including H1299 and A549 lung tumor cells, HeLa cervical tumor cells, Hct116 colon tumor cells, and DU145 prostate tumor cells using stable shRNA lentiviral vectors directed toward two different RGS17 target sequences (shRGS-1 and shRGS-2). Knockdown was confirmed using qRT-PCR (Fig. 2*A–C*). Knockdown was unsuccessful in HeLa and A549 cells; however, both shRNA constructs efficiently reduced RGS17 transcript to ~5% to 35% of its original level in H1299, Hct116, and DU145 cells. The construct shRGS-2 was the most effective in knockdown of RGS17 transcript, as measured by qRTPCR, as endogenous RGS17 protein was not measurable with tested antibodies. Cells seeded in culture at low density (500 cells per well of a 12-well tissue culture dish) were monitored for viable cell count by an MTT-based colorimetric assay throughout 6 to 10 days in culture (Fig. 2*A–C*). Both constructs greatly diminished the proliferative rate of tumor cells. In concordance with more effective knockdown, shRGS-2 was most effective in inhibiting proliferation. The degree of proliferative effect generally correlated with the degree of RGS17 knockdown in all cells tested. The proliferative effect of RGS17 knockdown as determined by MTT assay correlated well with decreased colony formation and decreased cell count in shRGS-2 cells, and the correlation of MTT values with cell numbers was similar between H1299-vector and H1299-shRGS-2 (Supplementary Fig. S2). Due to the consistency and robustness of the effect of RGS17 knockdown on H1299 and Hct116 cells, these cell lines were chosen for use in xenograft models of tumorigenesis. H1299 and Hct116 tumor cell lines with vector control or shRGS-2 were injected s.c. into athymic nude mice to monitor tumorigenesis (Fig. 2*A–B*). In both cell lines, knockdown of RGS17 significantly decreased tumor volumes measured after 4 to 5 weeks ($P > 0.01$). Knockdown in H1299 decreased the average tumor volume from 380 to 95 mm^3, whereas knockdown in Hct116 decreased the average tumor volume from 700 to 289 mm^3.

To evaluate the effect of RGS17 overexpression in tumor cells, we stably transfected H1299 with pCDNA3-3HA vector or pCDNA3 expressing NH_2-terminally 3HA-tagged RGS17. Cells expressing 3HA-RGS17 showed a 13.6-fold increase in total RGS17 transcript as measured by qRT-PCR (data not shown), and robust protein expression of 3HA-RGS17 as detected using HA antibody (Fig. 2*D*). Overexpression of RGS17 was found to enhance the proliferative rate of H1299 as measured by MTT assay over 11 days in culture (Fig. 2*D*). Differences in proliferation with overexpression were not as robust as with RGS17 knockdown, which may be expected in already highly proliferative tumor cells, which express endogenous RGS17 at increased levels over nonmalignant cells (Supplementary Fig. S1*B*).

RGS17 affects expression of CNS developmental, receptor-mediated cell signaling, and CREB-responsive genes. Having shown that RGS17 is commonly overexpressed in tumors and confers proliferative effects, we set out to define specific mechanisms through which RGS17 may act to confer such a proliferative phenotype. Exon microarray technology (Affymetrix Chip Human-Exon10ST) was used to delineate specific transcriptional effects of RGS17 expression in tumor cells, and to discover molecular pathways that may be affected by RGS17. RNA was isolated from H1299 cells with vector, shRGS-1 or shRGS-2, as well as Hct116 cells with vector or shRGS-2. These were used in microarray assays to identify genes that are differentially expressed upon loss of RGS17. Full results are included in Supplementary Table S1. With a cutoff of >1.4-fold differences in expression in at least 2 of the 3 biological triplicates and a P value of <0.05, we identified 52 genes that were differentially expressed with RGS17 knockdown. Only two of these genes, *FoxO4* and *Hnt*, were up-regulated in response to RGS17 knockdown. All other genes that met the inclusion criteria were down-regulated in response to RGS17 knockdown. RGS17 transcript itself was found to be reduced by 51% to 82% in microarray data for knockdown samples. To further investigate the gene expression pattern associated with RGS17 expression in tumors, an analysis of six published array data sets was performed to identify genes that are coexpressed with RGS17 in lung tumors. We performed a general regression test for each individual data set and also applied a linear mixed model test for three Affymetrix data sets and three cDNA array data sets, separately. Nineteen transcripts met our highest inclusion criteria by being found to be coregulated with RGS17 in both the individual data set test and the combined data sets test. Although the expression of genes indicated by this method may not be directly affected by RGS17, the expression profile generated may be useful in delineating what transcriptional activation pathways are frequently associated with high RGS17 expression in tumors.

All genes identified by the above methods were classified based on function by searching the Gene Ontology Annotation from the European Bioinformatics Institute (Supplementary Table S2).[6] The most common functional groupings of genes were those that function in the CNS and those associated with receptor-mediated cell signaling, with 56.3% of the affected genes belonging to one

[5] http://www.ncbi.nlm.nih.gov/sites/entrez?db=unigene

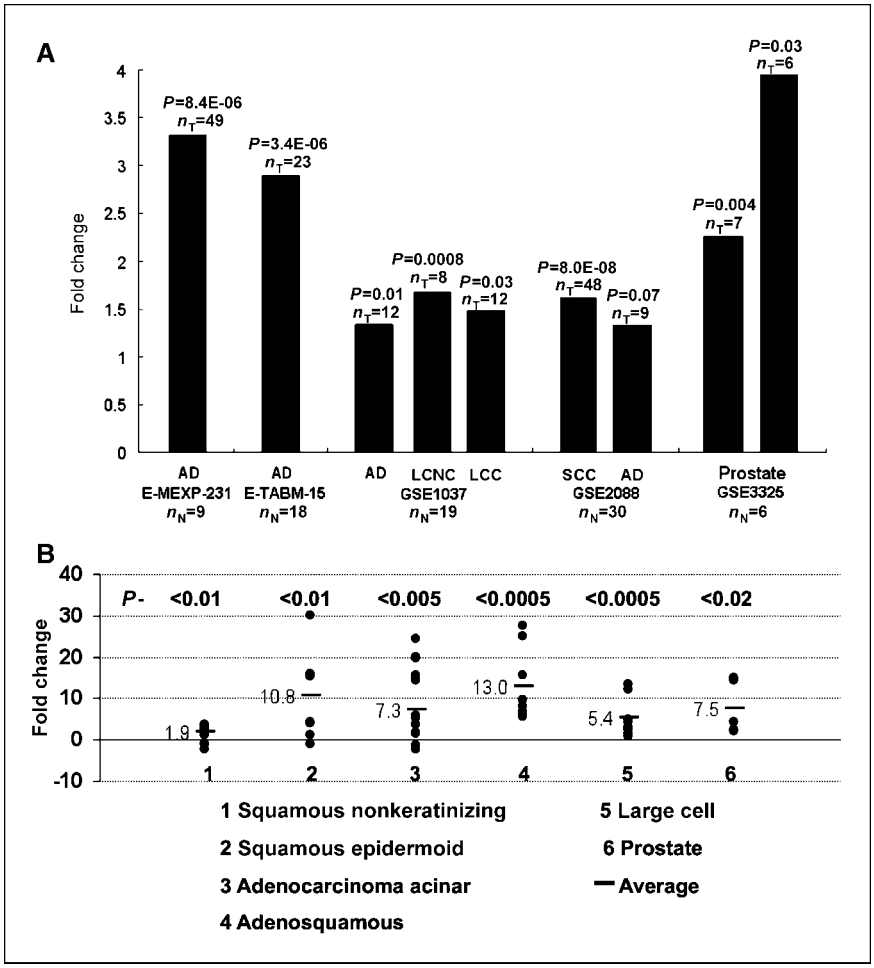

Figure 1. Overexpression of RGS17 in human cancers. *A,* in four published microarray data sets for lung cancer versus normal control tissue, and one for prostate cancer versus normal control tissue, RGS17 was highly expressed in tumor samples compared with controls. *AD,* adenocarcinoma; *LCNC,* large cell neuroendocrine carcinoma; *LCC,* large cell carcinoma; *SCC,* squamous cell carcinoma; *nN,* number of normal samples; *nT,* number of tumor samples. *P* values were calculated by two tailed Student's *t* test. *B,* qRT-CPR detecting RGS17 transcript accumulation in lung tumors of various pathologies and prostate tumors compared with patient-matched normal control tissue. RGS17 expression is induced in lung and prostate tumors. *IB,* immunoblot.

or both of these categories. Twenty-three genes (32%) of those listed in Supplementary Table S1 were identified as putative CREB-responsive genes. These genes were identified using the Salk Institute CREB Target Database (10). These genes have a conserved CREB-Responsive Element (CRE) in the proximal promoter and/or exhibit CREB binding in chromatin immunoprecipitation (ChIP)-on-chip analysis. Those genes with a conserved CRE and a ratio of ChIP signal over control genomic DNA of ≥ 2 (P <.001) are denoted in bold.

Microarray results for several of the strongest candidate CREB responsive gene products, including RIPK4, Protocadherin 7 (PCDH7), NR2F1, and FoxP2 were validated using conventional semiquantitative PCR and qRT-PCR (Fig. 3*A*). Expression of all of these CREB-responsive genes as well as CREB-responsive Cyclin D1 and KCIP-1 were found to be reduced with RGS17 knockdown by these methods. FoxO4, which was found in microarray data to be induced upon RGS17 knockdown, was also found to be induced in RGS17 knockdown cells by qRT-PCR. RGS17 expression itself was found to be decreased by 2.7-fold by qRT-PCR in these knockdown samples. Coexpression data were validated for KCIP-1 in colon and prostate tumors (Fig. 3*B*). Relative expression in tumors compared with matched normal tissues is higher in prostate but not in colon tumors for both RGS17 and KCIP-1. Pearson's correlation analysis of RGS17 induction versus KCIP-1 induction in tumors shows a close correlation between the expression of RGS17 and KCIP-1 yielding correlation coefficients of 0.84 and 0.86 for colon and prostate cancer, respectively.

To determine the effect of RGS17 loss on the ability of the adenylate cyclase activator forskolin to induce CREB-responsive gene expression, cells with vector or shRGS-2 were treated with either solvent control or forskolin (Fig. 3*C*). Loss of RGS17 resulted in a loss of forskolin induction of FoxP2, Cyclin D1, and KCIP-1. These results show that RGS17 does indeed play a role in the cAMP-CREB pathway as has been previously suggested (4), and that loss of RGS17 leads to decreased expression of and decreased forskolin induction of CREB-responsive genes.

RGS17 induces cAMP formation, PKA-dependent CREB phosphorylation, and proliferation through the cAMP-PKA pathway. To determine if cAMP-PKA activation can induce proliferation in lung tumor cell lines and if the proliferative effect of RGS17 is through the cAMP-PKA pathway, H1299 cells were treated with the adenylate cyclase activator forskolin and/or the PKA inhibitor H89. H1299 cells with vector or shRGS-2 knockdown were assayed for cAMP activity and for forskolin-induced cAMP accumulation (Fig. 4*A*). cAMP activity was reduced upon loss of RGS17 as was dose-dependent forskolin-induced cAMP accumulation (P < 0.0005). The level of phosphorylated CREB (phosphor-serine 333) was reduced with loss of RGS17 from a phospho-CREB to total-CREB ratio of 0.77 to 0.22. Under low

[6] http://www.ebi.ac.uk/GOA/

serum (0.1%), proliferation of H1299 cells with vector alone was induced by forskolin treatment compared with treatment with DMSO solvent as measured by MTT assay, whereas proliferation was not significantly induced in cells with RGS17 knockdown (Fig. 4*B*). Furthermore, cAMP accumulation was increased in cells overexpressing 3HA-RGS17 with or without forskolin stimulation ($P < 0.005$ and $P < 0.01$, respectively; Fig. 4*C*). Levels of cAMP in forskolin-treated cells were increased by overexpression of 3HA-RGS17 to an average of 1.44 pmol/well compared with 0.6 pmol/well in cells with vector alone. Cells overexpressing RGS17 showed a modest increase in phospho-CREB relative to total-CREB from 1.26 to 1.60 p-CREB to t-CREB (p/t) ratio as determined by western analysis. Thus, RGS17 positively regulates cAMP accumulation, CREB phosphorylation, and forskolin-induced proliferation in lung tumor cells.

Treatment with H89 induced growth arrest under 1% serum as measured by MTT assay in H1299 cells with either vector or shRGS-2 (Fig. 5*A*). H89 treatment for 6 days did not show general toxicity to H1299 cell monolayers in culture (data not shown). Western blotting showed a loss of CREB phosphorylation in both vector and shRGS-2 containing cells upon treatment with H89 (Fig. 5*B, left*). Phosphorylated CREB levels are similar in vector versus shRGS cells under starvation for 12 hours, presumably due to initial reduction of endogenous phospho-CREB in the vector cells. After 4 days on 1% serum with or without H89 treatment, shRGS-2 cells showed dramatically reduced levels of both total and phosphorylated CREB (Fig. 5*B, right*), suggesting that RGS17 may mediate a positive feedback loop to facilitate CREB biosynthesis. RGS17 overexpresion partially restored proliferation in H1299 cells under treatment with H89 as measured by MTT assay (Fig. 5*C*). Increased growth rate with RGS17 overexpression is more robust under 1% serum than previously observed under 10% serum. Western analysis shows that although H89 inhibits CREB phosphorylation in these cells, overexpresion of RGS17 partially protects CREB phosphorylation from inhibition by H89 (Fig. 5*D*). RGS17 overexpression limited the loss of phospho-CREB relative to total-CREB to 44% compared with 88% without RGS17 overexpression. RGS17 overexpression also increased levels of total CREB in H1299 cells. These results show that RGS17 is required for CREB phosphorylation and proliferation, and PKA activity and subsequent CREB phosphorylation are required for H1299 lung tumor cell proliferation under these conditions.

Discussion

Our observations show that cAMP-dependent PKA activation and CREB phosphorylation are important events in RGS17 induced proliferation in lung tumor cells. This is evidenced by our results demonstrating RGS17 and PKA-dependent CREB phosphorylation, RGS17 regulation of CREB responsive gene expression, and RGS17-dependent forskolin stimulation of growth. There are many CREB-responsive gene products that may be effectors of PKA-CREB activation, including Cyclin D1, RIPK4/PKK (protein kinase C–associated NFκB activator; ref. 11), and KCIP1 (antiapoptotic RGS17 interacting protein kinase C inhibitor), all of which we found to be affected by loss of RGS17. NFκB, which can be activated directly

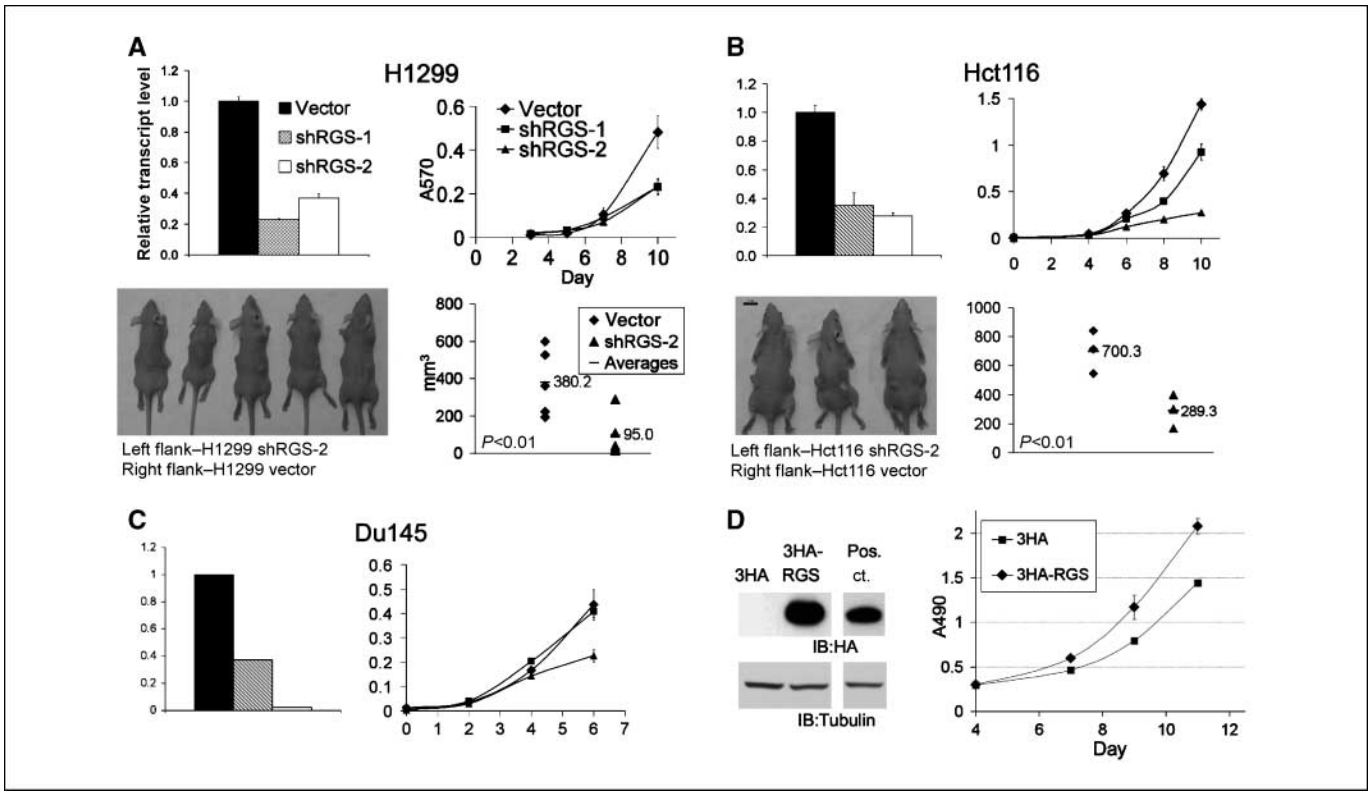

Figure 2. RGS17 is required for maintenance of proliferative rate of tumor cell lines. *A,* RGS17 transcript was measured by qRT-PCR. Proliferation was measured by MTT assay for several days after seeding at 500 cells per well. H1299 cells exhibit slowed growth and decreased tumor size in nude mice when RGS17 transcript is knocked down. Control cells were injected into the right flank of each mouse, whereas shRGS knockdown cells were injected into the left flank of each mouse. *B,* Hct116 cells show slowed growth and decreased tumor size in nude mice when RGS17 transcript is knocked down. *C,* DU145 cells show slowed growth when RGS17 transcript is knocked down. *D,* Western blot showing 3HA-tagged RGS17 overexpression in H1299 cells. RGS17 overexpression in H1299 cells increases growth rate as measured by MTT assay.

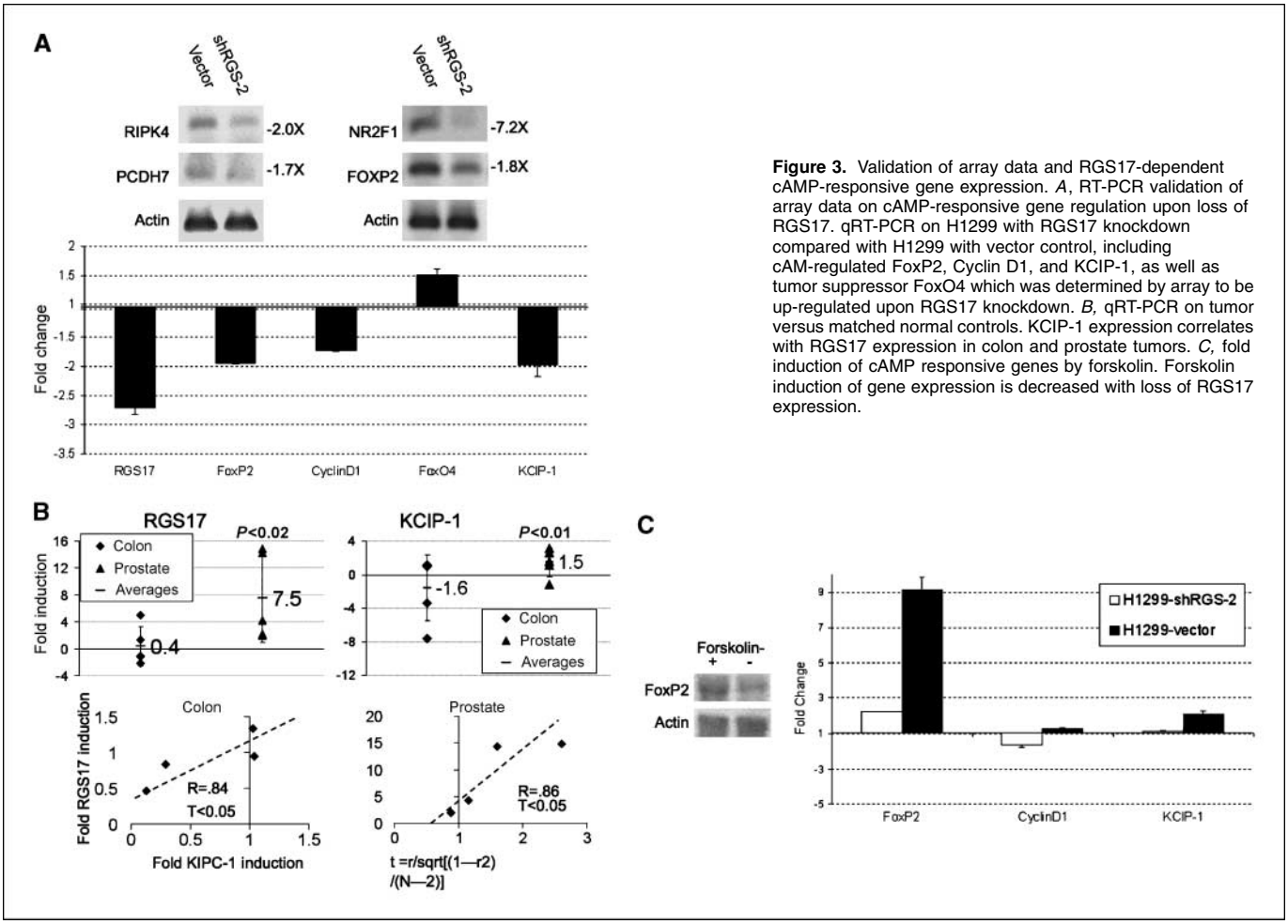

Figure 3. Validation of array data and RGS17-dependent cAMP-responsive gene expression. *A*, RT-PCR validation of array data on cAMP-responsive gene regulation upon loss of RGS17. qRT-PCR on H1299 with RGS17 knockdown compared with H1299 with vector control, including cAM-regulated FoxP2, Cyclin D1, and KCIP-1, as well as tumor suppressor FoxO4 which was determined by array to be up-regulated upon RGS17 knockdown. *B,* qRT-PCR on tumor versus matched normal controls. KCIP-1 expression correlates with RGS17 expression in colon and prostate tumors. *C,* fold induction of cAMP responsive genes by forskolin. Forskolin induction of gene expression is decreased with loss of RGS17 expression.

by PKA (12), may also be involved in the proliferative and survival effects of RGS17 independently of CREB. PKA activity in RGS17-expressing cells is likely to have proliferative and survival effects through one or more of these effectors. Delineation of the roles of these effectors in RGS17-mediated tumor cell proliferation requires further investigation.

CREB has been described as a proto-oncogene having proliferative and survival effects on myeloid progenitors and has been implicated in their transformation in acute myeloid leukemia (13). Furthermore, PKA and CREB have also been shown to play a role in the tumorigenesis of endocrine tissues, and various molecular aberrations in this pathway have been observed in endocrine tumors (14). In a recent study, phosphorylated CREB was found to be an early marker for lung adenocarcinoma and the tobacco carcinogen 4-(methylnitrosamino)-I-(3-pyridyl)-1-butanone (NNK) was found to induce phosphorylation of CREB in a time-dependent manner (15). Tumor-specific immunoreactivity to anti–phospho-CREB was detected in 43 of 47 human lung adenocarcinomas, suggesting that CREB-regulated gene expression is a critical event in lung carcinogenesis In another study, NNK was found to induce CREB phosphorylation in a PKA-dependent manner in human lung adenocarcinoma and small airway epithelial cells (16). Interestingly, this activation of the PKA-CREB pathway was partially abrogated by inhibition of EGF receptor (EGFR) signaling, suggesting crosstalk between these signaling pathways. EGFR is often overexpressed or mutated in lung cancers and can be transactivated by several G-protein–coupled receptors (17). Interestingly RGS17 expression has been found to be induced in rat astrocytes upon EGFR stimulation (18). A very recent study showed that EGFR and PKA pathways are involved in oxidant induced survival of type II alveolar cells (19). Given the importance of EGFR signaling to lung cancer and the role of PKA in EGFR signaling, enhancement of EGFR signaling by RGS17 through PKA in lung tumors is an attractive hypothesis.

Expression array analysis suggested that the expression of a variety of CNS and receptor-mediated signal transduction genes are coregulated with RGS17 expression. RGS17, being a RGS with expression and function in the brain, would be expected to be associated with genes of such function. Consistent with neurologic function, there is evidence that RGS17 may be involved in dopaminergic signaling. RGS17 and other RZ subfamily RGS proteins reduce D2R-mediated cAMP inhibition (4), and RGS17 transcript is decreased in dopamine D1 receptor knockout mice (20). Dopamine receptors are G-protein–coupled receptors that can up-regulate (D1R) or down-regulate (D2R) cAMP signaling (21). As mentioned in the introduction, RGS17 can also abrogate μ-opioid induced cAMP inhibition (8).

Interestingly, RGS17 knockdown resulted in a significant ($P < 0.05$) increase in expression of only the FoxO4 and Hnt genes, both of which have tumor suppressive roles. FoxO4 has known tumor suppressive functions through the activation of p27KIP (22, 23) and suppresses HER-2–mediated tumorigenicity (22). Hnt encodes Neurotrimin and is closely linked to its paralog opioid binding/

cell-adhesion molecule–like, which is frequently lost in ovarian cancer and has tumor-suppressor function. Repression of these tumor suppressors by RGS17, or a combination of this with activation of CREB-responsive genes may lead to, or may be necessary for the proliferation of tumor cells.

The results presented here identify RGS17 as a cAMP-PKA-CREB–activating regulator of lung tumor cell proliferation. Our observation that expression of RGS17 is widely up-regulated in tumors provide further evidence that RGS17 plays a role in tumorigenesis. Interestingly, we also found RGS17 to be consistently up-regulated in prostate tumors, in which a role for G-protein and PKA signaling has been implicated (24). The profound effect of loss of RGS17 and/or PKA inhibition on tumor cell growth establishes RGS17 and the cAMP-PKA-CREB pathway as potential targets of cancer therapeutics. Robust inhibition of both total and phospho-CREB in RGS17 knockdown cells accompanies a dramatic decrease in the growth rate of tumor cells and may likely be due to feedback autoregulation of CREB expression through CREs within the CREB promoter itself. Increased total CREB in RGS17 overexpressing cells also suggests a positive feedback mechanism of CREB transcriptional regulation, which has been well-documented (25, 26). Increased cAMP levels and proliferation are induced by overexpression of RGS17 in lung tumor cells. RGS17 overexpression is sufficient to promote proliferation, especially under low serum conditions, and partially rescue proliferation in cells under PKA inhibition. Because H89 inhibition of PKA cannot be expected to be 100% effective, we conclude that overexpresion of RGS17 overcomes inhibition through increased PKA activation rather than bypass through another pathway. Culture of lung tumor cells for 4 days on low serum reveal robust effects of RGS17 expression on proliferation, CREB phosphorylation and total CREB expression, indicating that sustained activation of CREB plays a critical role in RGS17 induced proliferation. These findings lead to a model for RGS17-induced proliferation where cAMP-PKA-CREB signaling is regulated by RGS17 through inhibition of adenylate cyclase inhibiting G(i)-coupled receptors permitting G(s)-coupled receptor signaling. Further investigation of the involvement of RGS17 and the cAMP-PKA-CREB pathway in receptor-mediated tumor phenotypes including those mediated by μ-opioid receptors and the recently genetically implicated nAChR family receptors on chromosome 15q will be vital to the better understanding of lung tumorigenesis. It will also be imperative to investigate

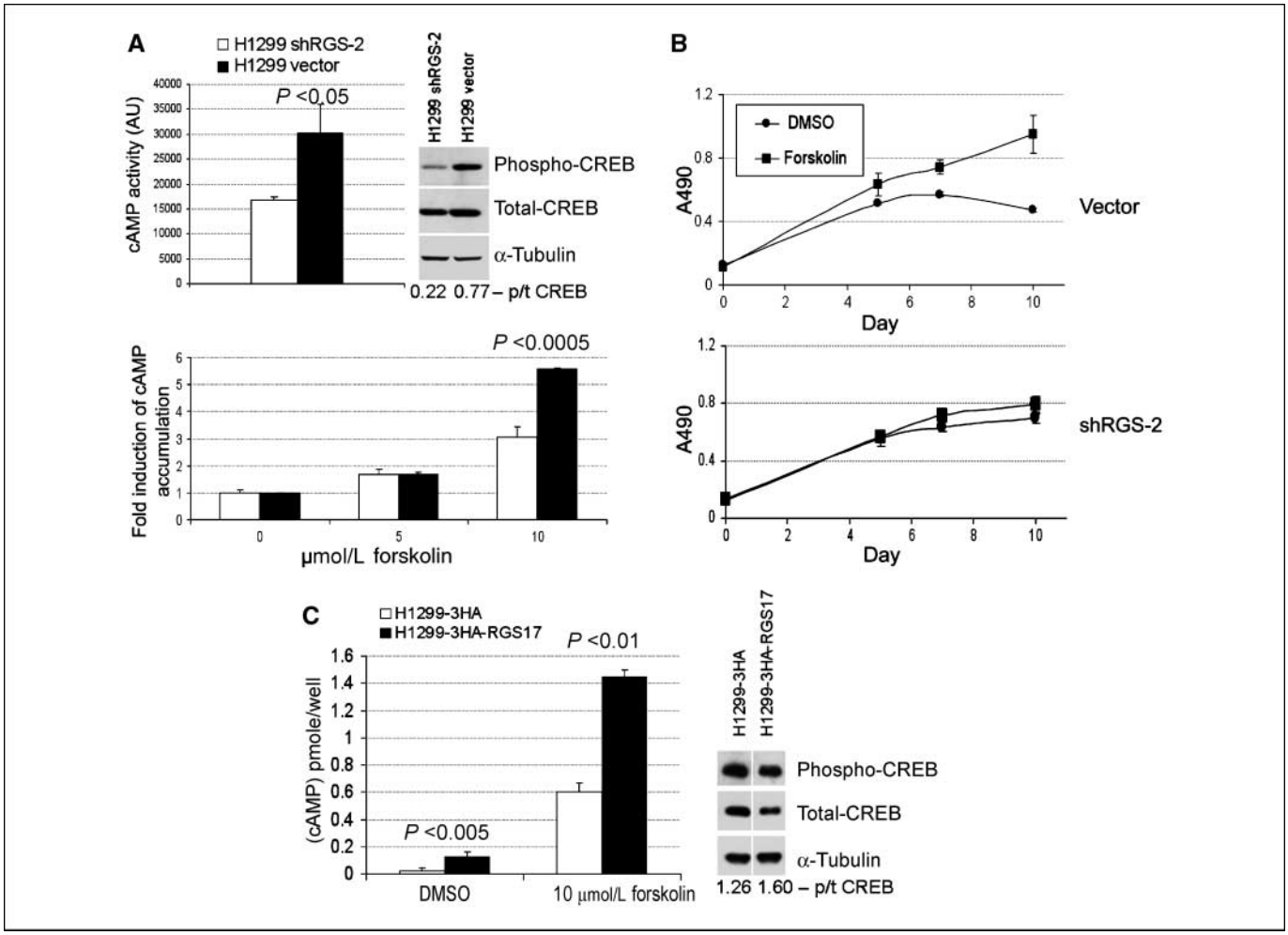

Figure 4. RGS17 induces cAMP formation, CREB phosphorylation, and growth stimulation by forskolin. *A,* cAMP activity in arbitrary units (*AU*) and the fold induction of cAMP formation by forskolin is decreased with loss of RGS17. Western blotting shows that CREB phosphorylation is lost with RGS17 knockdown. *p/t CREB,* ratio of phospho-CREB signal to total CREB signal. *B,* cells under 1% serum were treated with DMSO or 10 μmol/L forskolin and monitored for proliferation using MTT assay. RGS17 is required for forskolin stimulation of growth in H1299 cells. *C,* 3HA-RGS17 overexpression in H1299 cells increases cAMP levels and enhances forskolin induction of cAMP formation. Western blotting shows that 3HA-RGS expression modestly increases phospho-CREB levels in relation to total CREB.

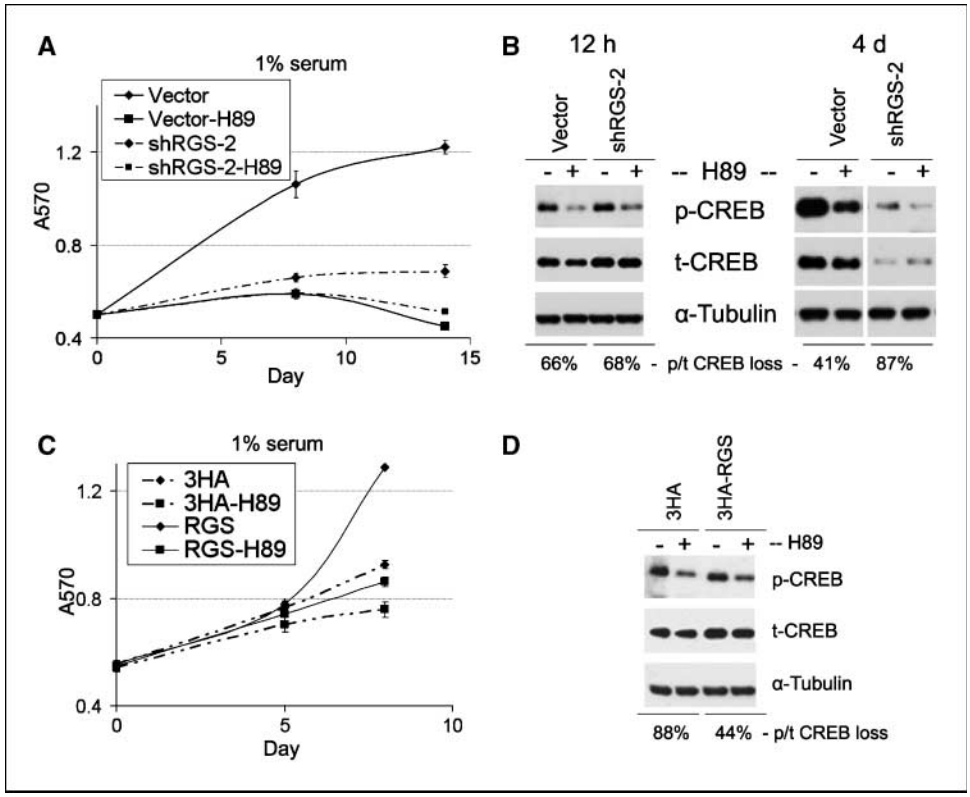

Figure 5. RGS17 overexpression protects against PKA inhibitor mediated inhibition of CREB phosphorylation and growth arrest. *A,* H1299 cells with vector or shRGS-2 were plated at low density (500 cells per well of 12-well dish) and allowed to grow under 1% serum with or without H89. H89 arrests cell growth in both vector and shRGS-2 cells. *B,* Western blotting shows that H89 causes decreased phosphorylation of CREB in both vector and shRGS-2 cells under 1% serum for 12 h. When cells are treated with 1% serum long term (4 d), total CREB and phospho-CREB are reduced in cells with RGS17 knockdown. *C,* overexpression of 3HA-RGS17 (*RGS*) protects H1299 cells from growth arrest induced by H89. *D,* Western blotting shows that CREB phosphorylation is inhibited by H89 and that 3HA-RGS17 overexpression partially protects CREB phosphorylation.

the roles of specific CREB target genes in RGS17 induced tumor cell growth.

Disclosure of Potential Conflicts of Interest

No potential conflicts of interest were disclosed.

Acknowledgments

Received 9/11/2008; revised 12/2/2008; accepted 12/4/2008; published OnlineFirst 02/24/2009.

Grant support: The Vanderbilt Microarray Shared Resource is supported by the Vanderbilt Ingram Cancer Center (P30 CA68485), the Vanderbilt Digestive Disease Center (P30 DK58404), and the Vanderbilt Vision Center (P30 EY08126).

The costs of publication of this article were defrayed in part by the payment of page charges. This article must therefore be hereby marked *advertisement* in accordance with 18 U.S.C. Section 1734 solely to indicate this fact.

Matched tumor and normal RNA was obtained from the SCC Tissue Procurement Core, Washington University, St. Louis, MO. We thank Weidong Wen, Washington University School of Medicine, Department of Surgery for performing all qRT-PCR reactions, the Tissue Procurement Core of Washington University (St. Louis, MO) for providing tumor tissues, and Qiong Chen for her help with various aspects of this study. All microarray experiments were performed in the Vanderbilt Microarray Shared Resource.

References

1. Rangel J, Nosrati M, Leong SP, et al. Novel role for RGS1 in melanoma progression. Am J Surg Pathol 2008; 32:1207–12.
2. Gu J, Wu X, Dong Q, et al. A nonsynonymous single-nucleotide polymorphism in the PDZ-Rho guanine nucleotide exchange factor (Ser1416Gly) modulates the risk of lung cancer in Mexican Americans. Cancer 2006; 106:2716–24.
3. Berman DM, Wang Y, Liu Z, et al. A functional polymorphism in RGS6 modulates the risk of bladder cancer. Cancer Res 2004;64:6820–6.
4. Mao H, Zhao Q, Daigle M, Ghahremani MH, Chidiac P, Albert PR. RGS17/RGSZ2, a novel regulator of Gi/o, Gz, and Gq signaling. J Biol Chem 2004;279:26314–22.
5. Berman DM, Gilman AG. Mammalian RGS proteins: barbarians at the gate. J Biol Chem 1998;273:1269–72.
6. Nunn C, Mao H, Chidiac P, Albert PR. RGS17/RGSZ2 and the RZ/A family of regulators of G-protein signaling. Semin Cell Dev Biol 2006;17:390–9.
7. Garzon J, Rodriguez-Munoz M, Lopez-Fando A, Sanchez-Blazquez P. The RGSZ2 protein exists in a complex with mu-opioid receptors and regulates the desensitizing capacity of Gz proteins. Neuropsychopharmacology 2005;30:1632–48.
8. Ajit SK, Ramineni S, Edris W, et al. RGSZ1 interacts with protein kinase C interacting protein PKCI-1 and modulatesμopioid receptor signaling. Cell Signal 2007; 19:723–30.
9. Chaparro J, Reeds DN, Wen W, et al. Alterations in thigh subcutaneous adipose tissue gene expression in protease inhibitor-based highly active antiretroviral therapy. Metabolism 2005;54:561–7.
10. Zhang X, Odom DT, Koo SH, et al. Genome-wide analysis of cAMP-response element binding protein occupancy, phosphorylation, and target gene activation in human tissues. Proc Natl Acad Sci U S A 2005;102:4459–64.
11. Meylan E, Martinon F, Thome M, Gschwendt M, Tschopp J. RIP4 (DIK/PKK), a novel member of the RIP kinase family, activates NF-κB and is processed during apoptosis. EMBO Rep 2002;3:1201–8.
12. Zhong H, Voll RE, Ghosh S. Phosphorylation of NF-κB p65 by PKA stimulates transcriptional activity by promoting a novel bivalent interaction with the coactivator CBP/p300. Mol Cell 1998;1:661–71.
13. Fischer H, Liu DM, Lee A, Harries JC, Adams DJ. Selective modulation of neuronal nicotinic acetylcholine receptor channel subunits by Go-protein subunits. J Neurosci 2005;25:3571–7.
14. Rosenberg D, Groussin L, Jullian E, Perlemoine K, Bertagna X, Bertherat J. Role of the PKA-regulated transcription factor CREB in development and tumorigenesis of endocrine tissues. Ann N Y Acad Sci 2002;968: 65–74.
15. Cekanova M, Majidy M, Masi T, Al-Wadei HA, Schuller HM. Overexpressed Raf-1 and phosphorylated cyclic adenosine 3′-5′-monophosphatate response element-binding protein are early markers for lung adenocarcinoma. Cancer 2007;109:1164–73.
16. Laag E, Majidi M, Cekanova M, Masi T, Takahashi T, Schuller HM. NNK activates ERK1/2 and CREB/ATF-1 via β-1-AR and EGFR signaling in human lung adenocarcinoma and small airway epithelial cells. Int J Cancer 2006;119:1547–52.
17. Daub H, Weiss FU, Wallasch C, Ullrich A. Role of transactivation of the EGF receptor in signalling by G-protein-coupled receptors. Nature 1996;379:557–60.
18. Liu B, Chen H, Johns TG, Neufeld AH. Epidermal

growth factor receptor activation: an upstream signal for transition of quiescent astrocytes into reactive astrocytes after neural injury. J Neurosci 2006;26:7532–40.
19. Barlow CA, Kitiphongspattana K, Siddiqui N, Roe MW, Mossman BT, Lounsbury KM. Protein kinase A-mediated CREB phosphorylation is an oxidant-induced survival pathway in alveolar type II cells. Apoptosis 2008;13:681–92.
20. Stanwood GD, Parlaman JP, Levitt P. Genetic or pharmacological inactivation of the dopamine D1 receptor differentially alters the expression of regulator of G-protein signalling (Rgs) transcripts. Eur J Neurosci 2006;24:806–18.
21. Banihashemi B, Albert PR. Dopamine-D2S receptor inhibition of calcium influx, adenylyl cyclase, and mitogen-activated protein kinase in pituitary cells: distinct Gα and Gβγ requirements. Mol Endocrinol 2002;16:2393–404.
22. Yang H, Zhao R, Yang HY, Lee MH. Constitutively active FOXO4 inhibits Akt activity, regulates p27 Kip1 stability, and suppresses HER2-mediated tumorigenicity. Oncogene 2005;24:1924–35.
23. Medema RH, Kops GJ, Bos JL, Burgering BM. AFX-like Forkhead transcription factors mediate cell-cycle regulation by Ras and PKB through p27kip1. Nature 2000;404:782–7.
24. Bagchi G, Wu J, French J, Kim J, Moniri NH, Daaka Y. Androgens transduce the Gαs-mediated activation of protein kinase A in prostate cells. Cancer Res 2008;68:3225–31.
25. Song H, Smolen P, Av-Ron E, Baxter DA, Byrne JH. Dynamics of a minimal model of interlocked positive and negative feedback loops of transcriptional regulation by cAMP-response element binding proteins. Biophys J 2007;92:3407–24.
26. Liu RY, Fioravante D, Shah S, Byrne JH. cAMP response element-binding protein 1 feedback loop is necessary for consolidation of long-term synaptic facilitation in Aplysia. J Neurosci 2008;28:1970–6.